Effects of the Atmosphere on Passive Microwave Sensing in the 20–100 GHz Region

W. H. CONWAY* AND G. A. LAROCCA†
Microwave Sensor Systems, Downey, Calif.

ONE of the newer methods of remotely sensing conditions of the environment is through passive microwave sensing, which can penetrate the atmosphere under a wide variety of environmental conditions. A need for relatively high spatial resolution suggests the use of the shorter microwave wavelengths for operation to keep requirements in physical aperture sizes to reasonable values. Present sensor state-of-the-art dictates the short-wavelength boundary of the useable spectrum to be in the order of 3 mm, while on the other end of the scale operational constraints on aperture size generally limit wavelength to be in the region of 3 cm. In this wavelength region atmospheric absorptions are caused by 1) resonance phenomenon of the atmospheric gases and 2) nonresonant processes, primarily water droplets in the form of rain, fog, and clouds. This Note briefly examines the causes of these two types of attenuations and their effects on the types of measurements that can be made. Fortunately, all is not as black as it may first appear, since the atmospheric absorption varies in this wavelength interval from an almost negligible value at the so-called atmospheric windows to virtually complete opacity at the very strong resonance absorption wavelength. This leads to totally different methods of obtaining remote sensing data, depending on whether the desired information concerns the atmospheric process or whether it concerns the terrestrial phenomenon underlying the atmosphere.

The main resonance absorption occurs at two frequency regions: a single line about 22.2 GHz and the region about 60 GHz (Fig. 1). The 22 GHz absorption is caused by pure rotational transitions of the water vapor molecules. The oxygen absorption occuring at 60 GHz is caused by a magnetic dipole resonance, having a series of fine structure levels associated with various rotational states of the molecule. Both of these resonance conditions exhibit pressure-broadened skirts. The oxygen absorption dominates, except in the immediate region of the water vapor line, even though the strengths of the two lines are in the same order of magnitude,

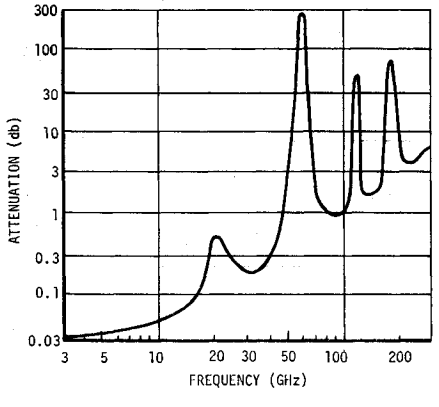

Fig. 1 Total vertical path attenuation vs frequency.

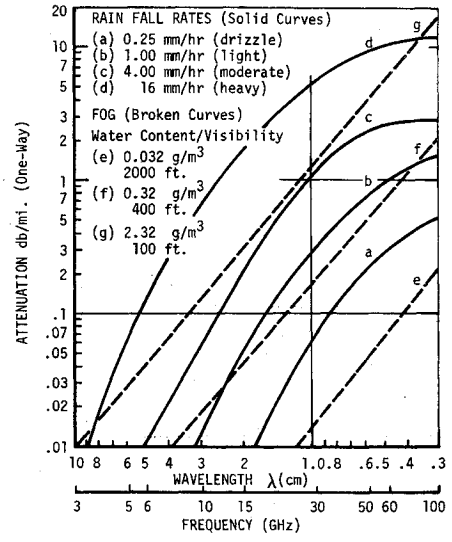

Fig. 2 Theoretical values of attenuation by rain and fog.

because of the much greater quantity of oxygen present in the atmosphere.

The attenuation caused by particles in the atmosphere can be attributed to two mechanisms. For fog and clouds, the mixture of water and air acts as a lossy dielectric and absorbs energy from the transmitted electromagnetic field. As the droplet size increases and rain falls, the medium acts less as a dielectric and more as a group of scattering spheres. The attenuation from each of these effects can be determined independently and linearly added. The analytical values of attenuation by rain (average rates in mm/hr) and fog are shown in the curve of Fig. 2 for various atmospheric conditions.

Thus, the magnitudes of the atmospheric attenuation encountered in the millimeter regions can vary from several tenths of a db in clear sky conditions to over 100 db at the oxygen absorption lines. The presence of weather in the window portion of the spectrum can add up to 3 or 4 db for practical conditions. Obviously, in the regions of the adsorptions, the small attenuations added by weather-related phenomena are always negligible compared to the primary absorption mechanism.

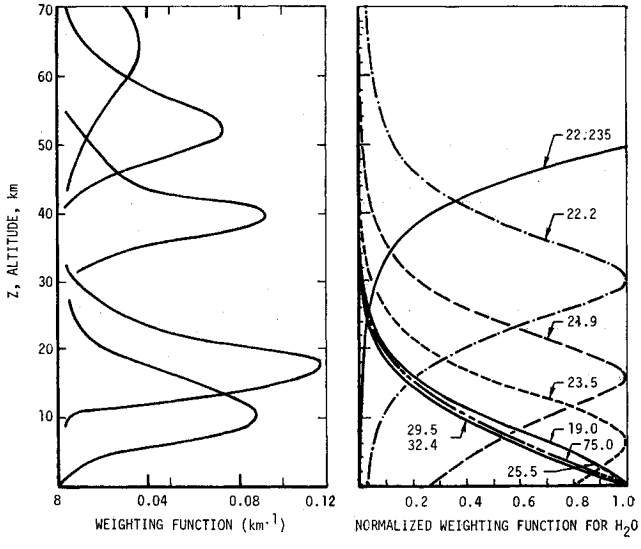

Fig. 3 a) Temperature weighting functions for nadir observations from space. These weighting functions each correspond to different frequency bands near 60 GHz.[1] b) Normalized weighting functions for interpreting water vapor opacity measurements in the terrestrial atmosphere.

Presented as Paper 70–198 at the AIAA 8th Aerospace Sciences Meeting, New York, January 19–21, 1970; submitted March 30, 1970; revision received May 28, 1970.

* Vice President.

† President.

Temperature Sounding

Staelin[1] has discussed the determination of atmospheric temperature profiles from satellite altitudes. The oxygen absorption occuring near 60 GHz is the basic measurement parameter. Data are taken at 6 frequencies along the skirts of the oxygen absorption lines and weighted to determine the temperature profile. In general, the weighting functions (e.g., Fig. 3a) are derived by calculating the height interval that contributes the most significant portion of the energy at any specific frequency. If the desired height measurement interval coincides with a weighting function interval, the atmospheric temperature can be obtained directly from a single radiometric measurement. However, the desired measurement height interval often is less than the weighting function interval or lies between two intervals. In this case weighting functions and the temperature measurement must be convoluted through an integral equation to determine the desired information. Staelin, indicates that this process can be used to provide information with errors as low as 1°–2°K throughout the majority of the atmosphere.

The effects of clouds and the underlying terrestial surface only appear in the weighting functions that peak very low in the atmosphere. Even then only a small percentage of the received radiation is contributed by error producing elements. A priori knowledge of the terrain temperature, even with reasonably broad uncertainties, can be used to reduce the error contribution to acceptably small levels.

This technique is presently being supported by NASA and hardware for flights in 1972–1973 is now in fabrication.

Cloud Location and Identification

For the measurement of absolute humidity and liquid water droplet content of the atmosphere, the water vapor attenuation near 22 GHz is the primary mechanism being measured. The computational techniques involved are a little more complicated than the temperature sounding techniques, since the distribution of water vapor in the atmosphere is not constant. Two variables must be separated, i.e., water vapor content and temperature. A set of water vapor interpretation weighting functions developed by Staelin is shown in Fig. 3b.

Knowledge of the temperature profile and water vapor content of the atmosphere can be used in conjunction with measurements made in the "window" portions of the microwave spectrum, to determine the cloud water droplet content. In this case a cloud looks very warm to a microwave radiometer. If the background temperature is known a priori or through measurements made at other frequencies, it is possible to determine the microwave density of the cloud. The attenuation of the cloud is related to the water droplet content by $\beta = M\ 10^2\ \lambda^2$ where β = microwave attenuation, M = integral multiplier, and λ = operating wavelength. Using this equation the water content can then be determined.

Kreiss[2] also discusses the influence of clouds on background brightness temperature. The case considered uses the sea surface as a background and shows brightness temperature increases due to clouds (at 19.35 GHz) ranging from 3.5° to 43°K. Signals of this magnitude should allow extraction of a considerable body of information from the radiometric measurement data. Several of the examples cited by Kreiss involve clouds that are actively raining. Under these conditions, the areas of rain showers appear as "hot" spots within the cloud, which itself appears warmer than the background sea. This also leads to the suggestion that other clouds exhibiting such "hot" spots may actually be caused by areas of showers within the cloud that never have the opportunity to emerge. It has previously been determined that clouds with high ice contents do not exhibit these characteristics and in fact appear relatively cool radiometrically. The ability to locate and identify cloud formations should prove of considerable use to the science of meteorology. This should be even more useful when correlated with data from other sensors in the optical and infrared region to allow determination of the rain content of a cloud, and possibly being able to penetrate multilayer cloud formations to obtain this data.

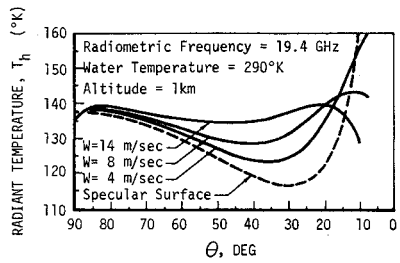

Fig. 4 Temperature of horizontally polarized radiation as a function of angle.

Horizon Sensing

For horizon sensing, if the operating frequency chosen is one that has a very high attenuation in the atmosphere, the transition from the very "cold" of outer space to the "warm" oxygen layer will be very uniform. Horizon sensing for purposes of vertical orientation reference using this type of sensor can be considered to be analogous to tracking the centroid of a very large target (the Earth's oxygen sphere). In this case the edges of the target are almost 180° apart in space. The tracking techniques that can be used are conical scan and sequential lobing schemes. In general, conical scanning would require mechanical methods, while sequential lobing can be accomplished all electronically. Prior investigations of the utility of microwave horizon sensing have been overshadowed by the extremely cumbersome and power-consuming equipment needed for the sensor. The recent introduction of all-solid-state instrumentation in the 60-GHz range will generate renewed interest in this technique.

Sea-State and Surface Temperature Measurements

The total radiation emitted from the sea surface is dependent upon the surface temperature T_w and emissivity. The amount of radiation (energy) received by a microwave radiometer for a given frequency interval and field of view depends upon 1) the radiation emitted from the surface being viewed, 2) the angle of incidence θ, 3) atmospheric effects upon this emitted radiation, and 4) radiation contributed by the atmosphere to the radiometer.

Theoretical calculations by Stogryn[3] based on Kirchoff's approximations of a rough finitely conducting surface, showed that significant apparent radiometric temperature changes can be observed in horizontally polarized signals‡ for changes in sea state and incidence angle (Fig. 4). Stogryn's calcula-

‡ The expressions, "horizontally" and "vertically" polarized signals, refer to the horizontal and vertical spatial components of the polarized signals that are received.

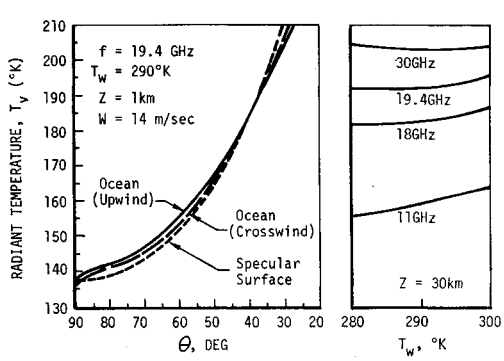

Fig. 5 Temperature of vertically polarized radiation vs angle and water temperature (left side). Radiometric temperature vs ambient temperature (right side).

tions further showed that for angles near 40° incidence to the water surface, vertically polarized radiometric temperatures are invariant with changes in sea state (Fig. 5, left side). Furthermore, it has been shown that the radiometric temperature is nearly insensitive to changes in the water thermometric temperature near the water resonance line (Fig. 5, right side). A frequency of 30 GHz was selected since the radiometric temperature is still essentially invariant to water temperature and at a frequency within an atmospheric window. It has been determined that any deviation from radiometric temperature invariance can be corrected by means of iterative computations.

In summary, the basis for performing sea state and sea temperature measurements using selected dual frequencies and orthogonal polarizations are 1) horizontally polarized microwave radiometric signals are significantly sensitive to changes in sea state and incidence angle (and in a lesser way to sea temperature); 2) vertically polarized microwave radiometric signals are invariant to sea state at or near an incidence angle of 40° to the surface; 3) microwave radiometric signals (of both polarizations) are nearly invariant to changes in the water thermometric temperature at frequencies at or near that of water absorption; and 4) the effects of nonpolarized loss mechanisms, like intervening atmosphere and foam, can be removed.

The method of removing the effects of non-polarized loss mechanisms that has been proposed by Aukland[4] et al. relies on the ability to generate a set of simultaneous equations with variables that are dependent on the sea state and parameters that are independent of the sea state. Solving these set of equations in effect allows the sea state conditions to be determined without overtly evaluating the attenuation contributed by the intervening atmosphere.

In a practical situation a curve will be generated relating radiometric attenuation. This in turn allows the data reduction process to be a simple set of tables on which values may be determined by direct "look-up." The nature of the sea is such that abrupt changes in sea state are rarely encountered. This fact in turn indicates that previous values of sea state can be used as a starting point in the search for the next value, further simplifing the data processing problem.

This technique of sea state measurement has been recently proposed with the result that considerable interest has been shown by the remote sensing community.

Summary

This paper treats the effect of the atmosphere on passive microwave remote sensing in a general summary nature. No attempt has been made to present an exhaustive technical treatment of the mechanisms involved in the atmospheric effects, nor to catalogue all of the possible applications related to this method of remote sensing. Recently, several special issues of technical journals have contained excellent treatises on these topics. Specfic reference is made to *Proceedings of the IEEE* special issue on Remote Environmental Sensing, April, 1969; *IEEE Transactions on Microwave Theory and Techniques* special issue on Noise, September, 1968 and *Proceedings of Symposium on the Remote Sensing of the Environment* sponsored by the University of Michigan.

References

[1] Staelin, D. H., "Passive Remote Sensing at Microwave Wavelengths," *Proceedings of the IEEE*, Vol. 57, April 1969, p. 427.

[2] Kreiss, W. T., "The Influence of Clouds on Microwave Brightness Temperatures Viewing Downwards Over Open Seas," *Proceedings of the IEEE*, Vol. 57, April 1969, p. 440.

[3] Stogryn, A., "The Apparent Temperature of the Sea at Microwave Frequencies," *IEEE Transactions on Antennas and Propogation*, Vol. AP-15, 1969, p. 278.

[4] Aukland, J. C. et al., "Remote Sensing of the Sea Conditions with Microwave Radiometer System," *Sixth Symposium on Remote Sensing of Environment*, Univ. of Michigan, Oct. 1969.

Subsonic-Hypersonic Aerodynamic Characteristics of Several Bodies of Revolution

Amado A. Trujillo*
Sandia Laboratories, Albuquerque, N. Mex.

Nomenclature

C_{AA} = forebody drag coefficient
$C_{N\alpha}$ = slope of normal force coefficient near $\alpha = 0°$, 1/deg
CP = fraction of model length from model nose to center of pressure
R = freestream Reynolds number based on model length
α = model angle of attack, deg

INTEREST in the aerodynamic characteristics of low-drag, high-volume re-entry vehicles, coupled with the paucity of this information for shapes other than cones, led to a series[1] of experimental and theoretical programs which sought to define drag, normal force, and static stability. The purpose of this Note is to summarize this work for four of these re-entry vehicle shapes. Sketches of the four fineness ratio 3 models, together with equations defining the model shapes, are shown in Fig. 1.

In 1952, Dennis and Cunningham[2] conducted tests at NACA on $\frac{1}{2}$- and $\frac{3}{4}$-power-law bodies and conical shapes with varying fineness ratios over a supersonic range of Mach numbers. More recently, Browne[3] tested $\frac{3}{4}$-power-law shapes with varying degrees of nose bluntness over the hypersonic Mach number range. At about the same time, Pousma[4] and Trujillo[5] of Sandia Laboratories tested seven configurations including $\frac{3}{4}$-power-law shapes with variations in nose bluntness, base corner rounding, and fineness ratio, as well as $\frac{1}{2}$-power-law, parabolic, and L-V Haack shapes. These tests were carried out over a range of Mach numbers from subsonic to hypersonic.

Theoretical studies on the configurations investigated experimentally by Pousma and Trujillo were carried out by Berman, et al.[6] and Franks.[7] Berman used an "exact" solution, while Franks used an "approximate" solution in calculating the aerodynamic characteristics. In addition, predictions were made using Newtonian impact theory.[8] Berman used the General Electric numerical flowfield solution. The solution in the nose region of a blunt body was carried out by direct transonic solution utilizing a streamline stepping technique in which computed shock wave shapes and body pressure distributions were compared with initially assumed values. A steady-state solution was carried out in the supersonic region, using the method of characteristics for both the pointed and blunt-nosed bodies. Franks' calculations were based upon a linearized method of characteristics program modified to accept the analytic descriptions of the models. In addition, he used other programs including blunt-body and conical-flow procedures to obtain initial-value data for the linearized method of characteristics program as well as aiding in the calculation of the geometric parameters required for the analytic body descriptions.

The experimentally and theoretically determined variations of $C_{N\alpha}$ and CP with Mach number for α near zero degree are presented in Fig. 1. For the configurations studied, the "exact" theory of Berman most accurately predicted the static stability coefficients. It is of interest to note that the Newtonian impact theory does offer a simple, and reasonably accurate, means of calculating the static stability of axisymmetric vehicles at hypersonic Mach numbers.

Received March 16, 1970; revision received May 25, 1970. This work was supported by the U.S. Atomic Energy Commission.

* Staff Member, Experimental Aerodynamics Division, Aerothermodynamics Projects Department. Member AIAA.